

Strain-Induced Anisotropic Spin-Density Distribution in $\text{La}_{1-x}\text{Sr}_x\text{MnO}_3$ Thin Films Revealed by Angle-Dependent X-Ray Magnetic Circular Dichroism

We have directly probed the anisotropy of the spin-density distribution in ferromagnetic $\text{La}_{1-x}\text{Sr}_x\text{MnO}_3$ (LSMO) thin films grown on SrTiO_3 (tensile) and LaAlO_3 (compressive) substrates by angle-dependent X-ray magnetic circular dichroism (XMCD) using a vector-type superconducting magnet. We found that the spin density is more preferentially distributed along the in-plane (out-of-plane) direction for the SrTiO_3 (LaAlO_3) substrate. This is consistent with the expectation from the epitaxial strain but is in contrast with previous X-ray linear dichroism results, which can be attributed to the preferential orbital occupation of the $3z^2 - r^2$ orbital in the surface magnetic dead layer.

$\text{La}_{1-x}\text{Sr}_x\text{MnO}_3$ (LSMO) is one of the most extensively studied perovskite-type oxides owing to its intriguing electric and magnetic properties such as colossal magnetoresistance and half-metallicity. It is well known that the physical properties of LSMO are significantly governed by the orbital occupation of Mn 3d bands. For example, LSMO ($x = 0.3$ – 0.5) thin films in the ferromagnetic (FM) metallic phase turn into antiferromagnetic (AFM) insulating phases under strong epitaxial strain from the substrates [1]. It has also been shown that the magnetic anisotropy of the FM LSMO thin films is dependent on the epitaxial strain: the magnetic easy axis is in-plane (out-of-plane) when the films undergo tensile (compressive) strain from the substrate [2, 3]. First-principles calculations have predicted that these phase transitions are associated with the preferential orbital occupation of the Mn $3d_{x^2-y^2}$ ($3d_{3z^2-r^2}$) orbital under tensile (compressive) strain [1]. However, previous X-ray linear dichroism (XLD) studies have shown that the $d_{3z^2-r^2}$ orbital is always preferentially occupied irrespective of the sign of the epitaxial strain, which has been attributed to the spatial symmetry breaking at the surface [4–6]. In the present study, we have directly observed the preferential orbital occupation of spin-polarized electrons in strained LSMO thin films via angle-dependent X-ray magnetic circular dichroism (XMCD). It is well known that one can deduce the spin magnetic moment (M_{spin}) from the spectral intensities of XMCD using a formula called the XMCD spin sum rule

[7]. It also includes an additional term called ‘magnetic dipole term’ M_T , which represents the spatial anisotropy of the spin-density distribution, i.e. the shape of the orbitals for the spin-polarized electrons [7–9]. Especially, one can extract the pure M_T component when M_{spin} is aligned perpendicular to the incident X-rays [so-called transverse XMCD (TXMCD) geometry] [9]. Here, we report on angle-dependent XMCD and TXMCD studies on ferromagnetic LSMO ($x = 0.3$) thin films grown on tensile SrTiO_3 (STO) and compressive LaAlO_3 (LAO) substrates, which has recently become possible by the use of a vector-type superconducting magnet [10].

We have grown LSMO ($x = 0.3$) thin films on tensile STO (001) and compressive LAO (001) substrates by laser molecular beam epitaxy [11]. Figure 1(a) shows the measurement geometry for the angle-dependent XMCD, with the definition of the angles of incident X-rays (θ_{inc}), applied magnetic field (θ_H), and magnetization (θ_M). In the present study, θ_{inc} was fixed at 45° and the field direction (θ_H) was varied. Figures 1(b) and 1(c) show the Mn $L_{2,3}$ -edge XMCD spectra for both the films measured at various values of θ_H . The XMCD intensity is approximately proportional to the spin magnetic moment M_{spin} projected onto the light axis ($\hat{p} \cdot M_{\text{spin}}$) [7]. The XMCD spectra change their signs around $\theta_H = -15^\circ$ – -20° for LSMO/STO and $\theta_H = -50^\circ$ – -55° for LSMO/LAO, showing that M_{spin} is directed nearly perpendicular to the incident X-rays around these values of θ_H . As shown by the expanded spectra in Fig. 2(a), however, there exist

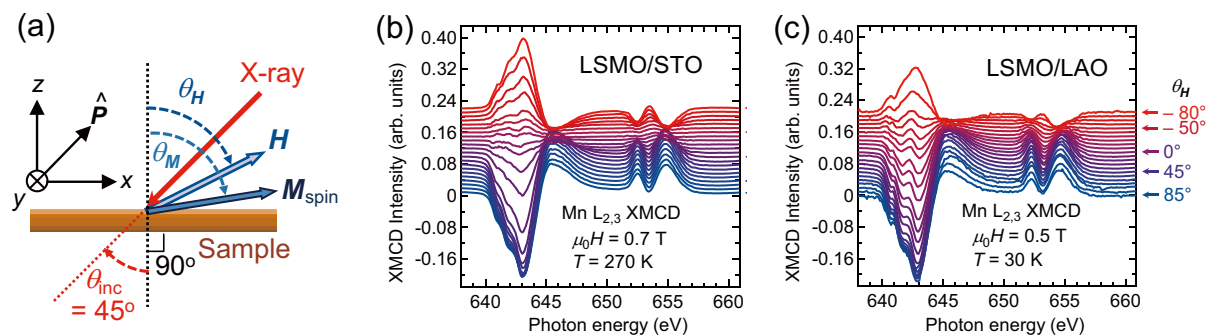


Figure 1: Angle-dependent X-ray magnetic circular dichroism (XMCD). (a) Schematic diagram of the experimental geometry with the definition of the angles of incident X-rays (θ_{inc}), magnetic field (θ_H), and spin magnetic moment (θ_M). \hat{p} is a unit vector along the incident X-rays. (b) (c) Mn $L_{2,3}$ -edge XMCD spectra for $\text{La}_{1-x}\text{Sr}_x\text{MnO}_3$ (LSMO) ($x = 0.3$) thin films grown on (b) tensile SrTiO_3 (STO) and (c) compressive LaAlO_3 (LAO) substrates.

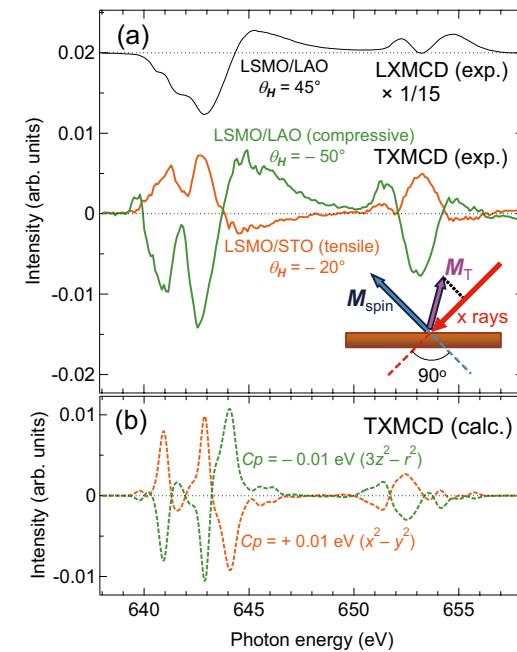


Figure 2: Transverse XMCD (TXMCD) spectra. (a) Experimental TXMCD spectra of the LSMO thin films grown on STO (orange) and LAO (green) substrates measured at $\theta_H = -20^\circ$ and $\theta_H = -50^\circ$, respectively. The black curve represents the longitudinal XMCD (LXMCD) spectra measured at $\theta_H = 45^\circ$. The inset shows a schematic drawing of the TXMCD geometry. (b) Calculated TXMCD spectra based on the Mn^{3+}O_6 cluster model with tetragonal symmetry. C_p denotes the strength of the tetragonal crystal field (the energy splitting between the $x^2 - y^2$ and $3z^2 - r^2$ levels is equal to $8C_p$) [14].

finite XMCD signals whose spectral line shapes are distinct from those at other values of θ_H [black curve in Fig. 2(a)], indicating that the observed spectra originate from the magnetic dipole moment M_T . Furthermore, as shown in Fig. 2(b), the experimental spectra can be well reproduced by the Mn^{3+}O_6 cluster-model calculation under tensile or compressive strain, suggesting that the obtained spectra arise from genuine TXMCD. Comparing the signs of the experimental TXMCD spectra with the calculated ones, it is demonstrated that the spin-density distribution of Mn in the LSMO/STO (LSMO/LAO) thin film is more $3d_{x^2-y^2}$ -like ($3d_{3z^2-r^2}$ -like), consistent with the expectation for the tensile and compressive epitaxial strain from the substrates.

Although the deduced anisotropic spin distribution is seemingly inconsistent with the results of previous XLD studies [4–6], this difference can be understood if one notices that XMCD is sensitive only to the spin-polarized electrons whereas XLD is sensitive to all the electrons. If the majority of the surface Mn atoms occupy the $3d_{3z^2-r^2}$ orbital but are not spin-polarized, the $3z^2 - r^2$ -like charge-density distribution at the surface and interface should be observed in the XLD measurements, while the $x^2 - y^2$ -like spin-density distribution from underneath layers should be observed in the XMCD measurements in the case of tensile strain. It is known that magnetic dead layers are formed at the surface and/or the interface of FM LSMO

thin films [12, 13]. The present angle-dependent XMCD and TXMCD studies, therefore, indicate close connection between the magnetic dead layer of LSMO thin films and the $3z^2 - r^2$ -like preferential orbital occupation at the surface.

The texts and figures in this article have been adapted from Ref. [15] with the authors' permission, based on the Creative Commons Attribution 4.0 International License.

REFERENCES

- [1] Y. Konishi, Z. Fang, M. Izumi, T. Manako, M. Kasai, H. Kuwahara, M. Kawasaki, K. Terakura, and Y. Tokura, *J. Phys. Soc. Jpn.* **68**, 3790 (1999).
- [2] F. Tsui, M. C. Smoak, T. K. Nath and C. B. Eom, *Appl. Phys. Lett.* **76**, 2421 (2000).
- [3] C. Kwon, M. C. Robson, K. -C. Kim, J. Y. Gu, S. E. Lofland, S. M. Bhagat, Z. Trajanovic, M. Rajeswari, T. Venkatesan, A. R. Kratz, R. D. Gomez and R. Ramesh, *J. Magn. Magn. Mater.* **172**, 229 (1997).
- [4] A. Tebano, C. Aruta, S. Sanna, P. G. Medaglia, G. Balestrino, A. A. Sidorenko, R. De Renzi, G. Ghiringhelli, L. Braicovich, V. Bisogni and N. B. Brookes, *Phys. Rev. Lett.* **100**, 137401 (2008).
- [5] C. Aruta, G. Ghiringhelli, V. Bisogni, L. Braicovich, N. B. Brookes, A. Tebano and G. Balestrino, *Phys. Rev. B* **80**, 014431 (2009).
- [6] D. Pesquera, G. Herranz, A. Barla, E. Pellegrin, F. Bondino, E. Magnano, F. Sánchez and J. Fontcuberta, *Nat. Commun.* **3**, 1189 (2012).
- [7] P. Carra, B. T. Thole, M. Altarelli and X. Wang, *Phys. Rev. Lett.* **70**, 694 (1993).
- [8] J. Stöhr, and H. König, *Phys. Rev. Lett.* **75**, 3748 (1995).
- [9] H. A. Dürr and G. van der Laan, *Phys. Rev. B* **54**, R760 (1996).
- [10] M. Furuse, M. Okano, S. Fuchino, A. Uchida, J. Fujihira, S. Fujihira, T. Kadono, A. Fujimori and T. Koide, *IEEE Trans. Appl. Supercond.* **23**, 4100704 (2013).
- [11] K. Horiba, H. Ohguchi, H. Kumigashira, M. Oshima, K. Ono, N. Nakagawa, M. Lippmaa, M. Kawasaki, H. Koinuma, *Rev. Sci. Instrum.* **74**, 3406 (2003).
- [12] K. Yoshimatsu, K. Horiba, H. Kumigashira, E. Ikenaga and M. Oshima, *Appl. Phys. Lett.* **94**, 071901 (2009).
- [13] M. Huijben, L. W. Martin, Y. -H. Chu, M. B. Holcomb, P. Yu, G. Rijnders, D. H. A. Blank and R. Ramesh, *Phys. Rev. B* **78**, 094413 (2008).
- [14] G. van der Laan, R. V. Chopdekar, Y. Suzuki and E. Arenholz, *Phys. Rev. Lett.* **105**, 067405 (2010).
- [15] G. Shibata, M. Kitamura, M. Minohara, K. Yoshimatsu, T. Kadono, K. Ishigami, T. Harano, Y. Takahashi, S. Sakamoto, Y. Nonaka, K. Ikeda, Z. Chi, M. Furuse, S. Fuchino, M. Okano, J. Fujihira, A. Uchida, K. Watanabe, H. Fujihira, S. Fujihira, A. Tanaka, H. Kumigashira, T. Koide and A. Fujimori, *npj Quantum Mater.* **3**, 3 (2018).

BEAMLINE

BL-16A

G. Shibata¹, M. Kitamura², M. Minohara², K. Yoshimatsu^{1,2}, T. Kadono¹, K. Ishigami¹, T. Harano¹, Y. Takahashi¹, S. Sakamoto¹, Y. Nonaka¹, K. Ikeda¹, Z. Chi¹, M. Furuse³, S. Fuchino³, M. Okano³, J. -i. Fujihira⁴, A. Uchida⁴, K. Watanabe⁴, H. Fujihira⁴, S. Fujihira⁴, A. Tanaka⁵, H. Kumigashira², T. Koide² and A. Fujimori¹ (The Univ. of Tokyo,²KEK-IMSS-PF,³AIST,⁴Fujihira Co., Ltd.,⁵Hiroshima Univ.)